Environmental Science
Processes & Impacts

Accepted Manuscript

ROYAL SOCIETY OF CHEMISTRY

rsc.li/process-impacts

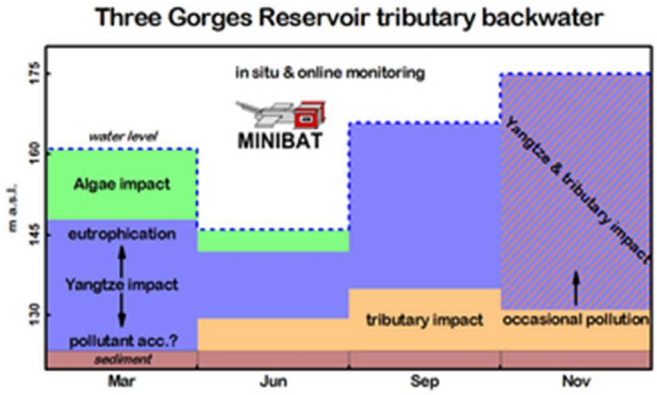

The current Three Gorges Dam management causes amplified pollutant transport from the Yangtze River main stream into its tributary backwaters.
28x17mm (300 x 300 DPI)

Environmental Science: Processes & Impacts

ARTICLE

Environmental water body characteristics in a major tributary backwater of the unique and strongly seasonal Three Gorges Reservoir, China

Received 00th January 20xx,
Accepted 00th January 20xx

DOI: 10.1039/x0xx00000x

www.rsc.org/

A. Holbach,*[a] Y. Bi,[b] Y. Yuan,[b] L. Wang,[c] B. Zheng,[c] and S. Norra[ad]

Ecological consequences of large dams, particularly regarding the Three Gorges Dam (TGD) on the Yangtze River in China, have been controversially and internationally discussed. Water quality within the Three Gorges Reservoir (TGR) has been deteriorated by highly underestimated eutrophication and algal blooms. Globally, the TGR is delineated from other comparable reservoirs by its low mean water residence time and its 30 m annual water level fluctuation. We used the in situ and online multi-sensor system 'MINIBAT' to analyse eight indicative physico-chemical parameters across depth and time within the Xiangxi River backwater, a representative major tributary of the TGR. The results revealed considerably changing environmental water body characteristics within the tributary backwater related to the TGR's typical seasonal hydroplogy. The Yangtze River main stream appeared to be the major contributor of dissolved and particulate water constituents within the Xiangxi River backwater. Eutrophication problems in spring and summer seasons are likely a consequence of extensive water mass exchange and pollutant transport processes in autumn and winter. In particular, the stratified water column shows varying layered impacts of the Yangtze River main stream and the Xiangxi River headwaters. This is a clear indication of a complex stratified flow pattern within this TGR tributary backwater. In our study, a major driver for the Yangtze River main stream impact was the rising TGR water level. The TGR's globally unique characteristic has thus become a central part of the recent eutrophication and pollution problem within the TGR. Herefrom, we deduced a proposal for an adapted dam management strategy.

Environmental Impact:

This paper aims at identifying environmental water body characteristics within a major tributary backwater of the Three Gorges Reservoir in China, particularly with respect to its pronounced typical seasonality. This reservoir is highly threatened by eutrophication problems and is unique in terms of its low mean water residence time and 30 m annual water level fluctuation scheme. We applied state-of-the art in situ and online multi-sensor monitoring techniques and identified the large water level fluctuation as a main driver of pollutant transport into the TGR tributary backwaters. These are extremely vulnerable to algal blooms. An adapted dam management strategy, based on a feedback with the current main stream pollution state, is proposed to reduce pollutant input into tributary backwaters.

1. Introduction

Since decades, the construction of large dams and reservoirs has been controversially discussed while dam planning and construction goes on as always. Without doubt, China is the leading nation in building dams. Almost 50% of the world's more than 45,000 large dams have been built in China.[1] Even though there are much larger dams and reservoirs in the world, the planning and construction of the Three Gorges Dam (TGD) on the Yangtze River was accompanied by exceptional international controversies and criticism. Indeed, the Three Gorges Reservoir (TGR) is an exceptional study area in the world with unique properties. In terms of size, mean water residence time, climatic zone, and mixing properties only the Itaipú Reservoir impounded on the Paraná between Brazil and Paraguay shows comparable properties as the TGR (**Error! Reference source not found.**, **Error! Reference source not found.**). However, the TGR is subject to 30 m annual water level fluctuation and is seriously eutrophic, whereas the water level in the oligotrophic Itaipú Reservoir only fluctuates less than 1 m per year.

The final stage of the TGR's impoundment with water levels ranging between 145 and 175 m above sea level (a.s.l.) has been reached since 2010. The huge impounded area is now

[a] *Institute of Applied Geosciences, Karlsruhe Institute of Technology, Kaiserstraße 12, 76131 Karlsruhe, Germany. Email: andreas.holbach@kit.edu; Fax: +49-721-608-47247; Tel: +49-721-608-47613.*
[b] *Institute of Hydrobiology, Chinese Academy of Sciences, 430072 Wuhan, China.*
[c] *Chinese Research Academy of Environmental Sciences, 100012 Beijing, China.*
[d] *Institute of Geography and Geoecology, Karlsruhe Institute of Technology, 76131 Karlsruhe, Germany.*
† Electronic Supplementary Information (ESI) available. See DOI: 10.1039/x0xx00000x

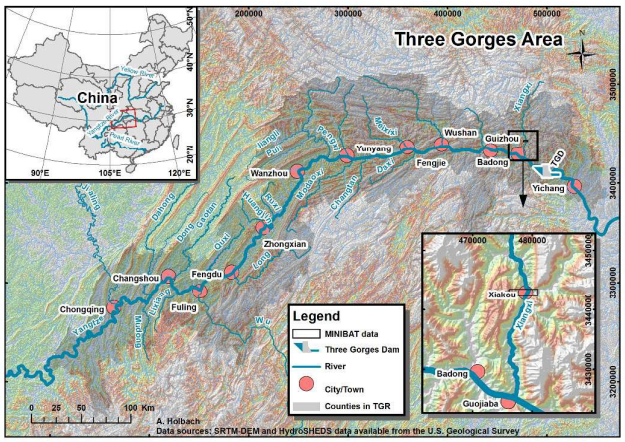

Fig. 1 Outline of the Three Gorges Reservoir, its location within China and the Xiangxi River backwater study area. Coordinates of the upper left overview map of China are in WGS84 system; other coordinates are in UTM zone 49 easting and northing format.

forming the more than 600 km long, partly more than 120 m deep, and markedly dendritic TGR (Fig. 1). So far, the main intentions of the TGD have been achieved: 1.) The TGD is protecting the downstream regions from devastating Yangtze River floods that have caused more than 300,000 deaths in the 20th century alone;[2] 2.) The world's largest hydropower plant is now generating around 85,000 GWh/year[5] accounting for around 1.8% of China's electricity consumption in 2012;[6] 3.) The navigation along the Yangtze River is now possible for 10,000 t vessels from Shanghai up to Chongqing and the transported cargo across the TGD river section has increased from around $10*10^6$ t before the dam construction[2] to $88*10^6$ t in 2010.[3] However, the reservoir impoundment has fundamentally changed the ecological conditions and has also caused severe environmental hazards.[7] Particularly eutrophication was highly underestimated by the conducted environmental impact assessments and now becomes visible by frequent algal blooms. These pose a serious threat to the utilization of the TGR as drinking water and fisheries resource and have already been directly addressed by numerous scientific studies.[4,8,9] Further, there are creeping environmental hazards with long-term effects caused by pollutant transport, accumulation, and/or mobilization in/from the reservoir sediments. These have been less frequently studied so far[9,10,11] and synoptic conclusions on a reservoir scale are still missing for the TGR. In the long-term, however, these can be equally serious as algal blooms as the massive capture of sediments in the Yangtze River reservoirs has already been proven.[12,13]

The presence of thermal density stratification in the TGR tributary backwaters was shown in several experimental field studies[4,9,14] as well as predicted by various modelling approaches[15,16]. One numerical modelling study even predicts the temporal occurrence of thermal stratification within the Yangtze River main stream of the TGR.[17] However, water body stratification alone does not represent any environmental threat at all but the correlated physico-bio-chemical processes taking place, such as the formation of algal blooms and pollutant transport processes. These can lead to problematic changes of water properties. In this field, several studies have pointed out the importance of processes in between the TGR tributary backwaters and the Yangtze River main stream. It was shown that the Yangtze River main stream in the TGR is characterized by higher concentrations of nutrients (N, P) and that import processes from the main stream into tributary backwaters are major drivers for eutrophication problems, there.[18,19] In particular, extensive field studies have identified density currents and related three-dimensional hydrodynamics as major nutrient and pollutant pathways as well as a regulating factor for the formation of thermal stratification suitable for algal blooms.[4,9,13,14] The corresponding nutrient transport, stratification and algal growth phenomena have also been numerically modelled with three-dimensional hydrodynamic approaches.[20,21] However, nutrients, eutrophication and algal blooms are only part of the story and a more generalized approach is necessary to capture other problematic processes, such as heavy metal transport and accumulation as well. For the TGR, balances of fates and pathways of heavy metals are so far missing in both field and modelling studies.

Throughout the year, the TGR water bodies are subject to four distinctive typical hydrological periods. In this study we applied state-of-the-art multi-sensor monitoring techniques to identify temporal distributions of physico-chemical water body characteristics within the impounded valley of the Xiangxi River, a major TGR tributary backwater (Fig. 1), throughout those typical hydrological periods. Therefore, we used a MINIBAT multi-sensor probe[9,22] to assess depth profiles of eight indicative physico-chemical parameters in this water body. Further information from this basic dataset was derived mathematically. With particular respect to the above mentioned environmental threats (eutrophication, nutrients, heavy metals), the dataset was analysed to outline stratification patterns in the water body, as well as impact ranges on the chemical composition of the water of both the Yangtze River mainstream and the Xiangxi River headwater on environmental characteristics of different layers. Further, changes of water body characteristics within the backwater itself were also of major interest. Getting back to a global perspective and the TGR's hydrological uniqueness we further extracted corresponding unique characteristics to be found within its water bodies. Conclusions will be drawn regarding challenges for water quality control within the TGR itself but also for possible dam management strategies, in general.

2. Materials and Methods

2.1. Typical and distinctive annual hydrological periods in the TGR

The water level in the TGR is subject to the specific management of the TGD and is meant to seasonally fluctuate between 145 and 175 m a.s.l.. Climate in the catchment of the TGR is associated with the East Asian summer monsoon.[23] Hence, the Yangtze River exhibits strong runoff seasonality with maximum inflows into the TGR (>70,000 m^3/s) in July and

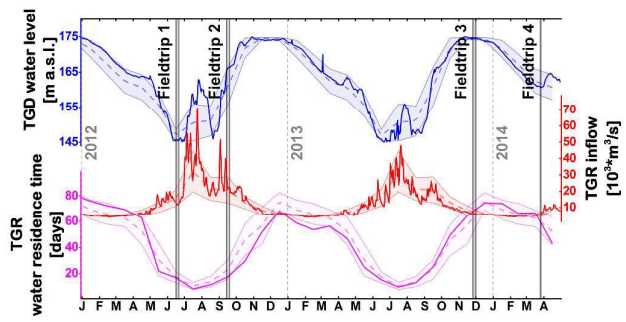

Fig. 2 Hydrological conditions in the TGR around our four conducted fieldtrips in the Xiangxi River backwater. Daily TGD water levels,[24] TGR inflows,[24] and corresponding calculated monthly TGR water residence times[5,24] are plotted above monthly (01.2010-04.2014) means±σ (dashed lines ± shaded areas).

minimum values (3,500-7,600 m³/s) from December till March.[24] In this context, the TGD is operated to maximise benefits for flood protection and electrical energy generation:

To ease summer discharge peaks and to avoid another devastating Yangtze River flood the TGR water level is kept at a low level during the flood season from June till August. This ensures a large flood retention volume within the TGR but reduces the energy yield of the hydropower plant in the TGD. The maximum outflow can be buffered by the reservoir and the TGD management resulting in maximum outflows of less than 50,000 m³/s.

During September and October the reservoir is filled up to its peak water level of around 175 m a.s.l.. This reduces the flood retention volume but increases the energy yield of the hydropower plant. The high water level phase from November till December is then followed by a water level drawdown from January till June. Consequently, four distinctive and typical hydrological scenarios are induced by the TGD management: Low water level, rising water level, high water level, and falling water level (Fig. 2).

The monthly TGR water residence time (T_R) was calculated based on arithmetic mean values of daily TGD outflows (Q_{TGD})[24], as well as water levels at the TGD (WL_{TGD}). Therefore, mean monthly volumes of the TGR water body (V_{TGR}) were linearly estimated from its minimum and maximum volumes (V_{min}: $22.15*10^9$ m³; V_{max}: $39.3*10^9$ m³),[5] respectively water levels (WL_{min}: 145 m a.s.l.; WL_{max}: 175 m a.s.l.).[24]

$$T_R = V_{TGR}/Q_{TGD}$$

$$V_{TGR} = V_{max}-(WL_{max}-WL_{TGD})*(V_{max}-V_{min})/(WL_{max}-WL_{min}).$$

Hydrological scenarios in the TGR are systematically repeated on a yearly basis and thus represent the 'normal' hydrological conditions within the TGR. The conditions within the four fieldtrips of this study were well within this normal range (monthly means±σ for the timeframe 01.2010-04.2014 in Fig. 2) of seasonally changing conditions. In turn, our acquired dataset can provide knowledge on the environmental water body characteristics during 'normal' conditions, but it can definitely not represent all kinds of possible conditions that may else occur, in particular not exceptional extreme events. These needed to be addressed from permanent long-term monitoring data.

Table 1 Hydrological scenarios during the four MINIBAT fieldtrips.[5,24]

		Mar	Jun	Sep	Nov
TGR inflow [m³/s]	*Min.*	5,300	11,600	21,500	5,800
	Max.	5,450	13,000	30,500	6,200
TGD Water level [m a.s.l.]	*Min.*	160.7	145.5	165.1	174.6
	Max.	160.9	145.7	166.3	174.7
Water residence time [days]	*Min.*	67.0	21.7	16.2	61.3
	Max.	67.2	22.8	18.6	85.2

The Xiangxi River, a typical one of 40 major tributaries of the TGR, enters the Yangtze River approximately 40 km upstream of the TGD.[25] Periodic water level fluctuations of the TGR form an impounded backwater that reaches 30-40 km upstream into its dendritic long channel-like former valley.

We performed measurements with a MINIBAT multisensor probe (2.2) within this backwater during four fieldtrips in the years 2012-2014. We have covered four very typical and very different hydrological scenarios by one of these fieldtrips each (Fig. 2, Table 1). During all fieldtrips our base was always in the town Xiakou located approximately 20 km upstream of the Xiangxi River confluence with the Yangtze River main stream (Fig. 1). Hence, this section of the Xiangxi River was covered almost daily by MINIBAT measurements during the four fieldtrips. Further, it is permanently located in the midst of the TGR backwater (Fig. 3) and reveals water depths of around 20 m in summer and 50 m in winter. This area turned out to be ideal to study patterns of environmental water body characteristics in the Xiangxi River backwater under the typical and different hydrologic conditions.

2.2. The MINIBAT underwater multisensor probe and recorded data

The MINIBAT is a multisensor probe for in situ and online measurements of relevant physico-chemical parameters in water bodies.[22] The MINIBAT has already been successfully applied within the TGR.[9,14] It is directly connected to a computer on a boat by a data transmission cable. The advanced MINIBAT system is equipped with sensors for eight physico-chemical indicative parameters of environmental conditions in the water (**Error! Reference source not found.**) as well as with a rack of five remote-control 50 mL water samplers. Physico-chemical parameters are highlighted individually in the following section. The parameters are recorded with 5 Hz frequency; for subsequent data evaluation we used one dataset per second. We obtained the corresponding GPS and bathymetry data from a Garmin GPSMAP 521s Chartplotter that was coupled with a depth sounder on the boat. A pressure sensor on the MINIBAT was used to determine its depth under water. The MINIBAT can be applied from a boat in two ways: 1.) it can be dragged through the water by the boat with 5-10 km/h and steered to different depths up to approximately 30 m by the use of its remote controlled wings; 2.) it can also be used as a vertical profiling probe to reach larger depths when the boat does not move.

The MINIBAT raw data was recorded during four fieldtrips along the whole Xiangxi River backwater. From this vast dataset a subset was selected from a very small horizontal area (31.12±0.05°N) that equals around 1 km of the Xiangxi River backwater around Xiakou (Fig. 1, Fig. 3). Remaining horizontal distances between measurement points were thus neglected during further data evaluation. Instead, we considered all analysed physico-chemical parameters *i* as functions *i*(*d*, *t*) of both depth below water surface *d* and time *t*. Additionally, we selected the deepest measurements of the MINIBAT depth profile recorded at the most upstream location of the Xiangxi River backwater of each fieldtrip to approximate water quality conditions of the Xiangxi River headwater (Fig. 3). The deepest points from the MINIBAT depth profile in the Yangtze River main stream were selected similarly to approximate water quality conditions of the Yangtze River main stream. In March 2014, however, we could not perform MINIBAT measurements in the upstream Xiangxi River backwater.

2.2.1.Indicative physico-chemical parameters directly measured with the MINIBAT

Technical specifications of all sensors applied in this study can be found in **Error! Reference source not found.**.

Temperature (T): T is a fundamental physical property of water. It controls its aggregate state as well as its density and is thus, particularly in freshwater, the driving force of water body stratification. Further, kinetics of bio-chemical processes generally depend on T.

Electrical conductivity (EC): The electrical conductivity of water is mainly related to its salinity and T. After standardization to 25°C, $EC_{25°C}$ [µS/cm] is consequently often used as a proxy for salinity (Sal) [ppm]:

$$Sal = EC_{25°C} * f, \text{ where } 0.5 < f < 0.7.$$

Here, we used $f = 0.64$.[26] Further, $EC_{25°C}$ is often a good conservative tracer through water mass mixing processes.[27]

Coloured Dissolved Organic Matter (CDOM): The sensor used here measures the fluorescence signal of water at 470 nm wavelength after excitation with 325 nm. Under these conditions, mainly humic-like substances are detected which are "derived from break-down of plant material by biological and chemical processes in the terrestrial and aquatic environments".[28] These can be of both natural and anthropogenic origin. In particular, organic compounds of urban sewage water exhibit corresponding fluorescence signals.[28] CDOM can therefore be a tracer of water masses and indicate e.g. sewage water sources. Light attenuation by CDOM can also have major impacts on the light environment in water bodies.

Turbidity (Turb): Turb of water is caused by colloids and suspended particles. Light attenuation caused by Turb can have major impacts on the light environment in water bodies. After verification, Turb can further serve as a proxy for the content of suspended particulate matter (SPM).

Chlorophyll *a* (Chl_a): Here, *in vivo* Chl_a concentrations were estimated from the fluorescence signal at 696 nm wavelength after excitation with 465 nm. Chl_a is the primary pigment of all photosynthetic organisms including all types of planktonic algae. The analysed Chl_a concentrations are thus a good proxy for algae abundance in general. Algal blooms, in particular excessive growth of toxin producing cyanobacteria, are a widely present serious risk for drinking water supply.

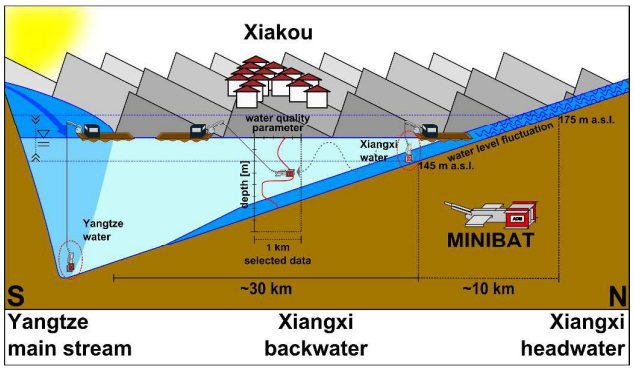

Fig. 3 Schematic illustration of in situ and online MINIBAT measurements in the Xiangxi River backwater used in this study. Note: seasonal water level fluctuation between 145 and 175 m a.s.l. determines upstream monitoring boundaries for the MINIBAT. For geographic reference see Fig. 1.

Oxygen saturation (O_2%): In water, O_2 is produced by algal photosynthesis and consumed by aerobic respiration of organisms. An equilibrated water/air interface would always form 100% O_2%. Corresponding over- or undersaturation is caused by the above mentioned bio-chemical processes. Anoxic conditions can occur due to little vertical turbulence. This is problematic for aerobic organisms and can further lead to microbial production of CH_4, toxic H_2S, and the release of pollutants from sediments.

pH (pH): In natural waters pH depends on geogenic environmental settings of the watershed and anthropogenic impacts. Within natural open water bodies mainly photosynthesis, respiration, and assimilation of nitrogen cause vertical gradients and temporal changes of pH.[29] PH is further critical for the mobility and bioavailability of numerous pollutants.

Photosynthetically active radiation (PAR): This parameter covers the range of visible light between 380-570 nm wavelengths and was measured as photon flux density. From two simultaneously measured PAR values we derived the euphotic depth (d_{eu}) where underwater PAR dropped to only 1% of the above water PAR.[29]

2.2.2.Parameters derived from MINIBAT data and water samples

Suspended particulate matter (SPM): Additionally to the monitored MINIBAT parameters, numerous water samples were also taken at selected sites throughout the study area and during all four fieldtrip times. Here, analyses of SPM concentrations are used to study the Turb/SPM relationship. Specific results of other water constituent analyses will be dealt with in another coming paper. From water samples (V ≈ 50 mL) SPM was separated with previously weighed filters (Sartorius Stedim cellulose acetate membrane; pore size: 0.45 µm; diameter: 25 mm). These filters were air dried and

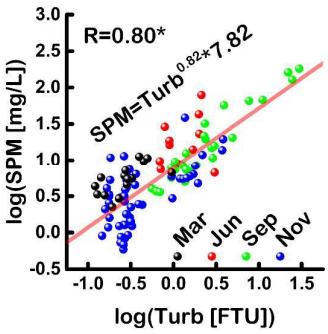

Fig. 4 Scatter plot of log(SPM) versus log(Turb) with least squares linear fit function. Pearson correlation coefficient (significant at a 0.05 level) and the fit function formula are plotted explicitly.

sealed before being weighed again. The SPM concentration was calculated as follows:

$$\mathrm{SPM} = (w_L - w_0)/\mathrm{V}_f.$$

Here, w_0 is the raw filter weight, w_L is the loaded filter weight, and V_f is the filtered water sample volume. With respect to water density, the density of quartz (2.56 g/cm^3) is commonly used to estimate SPM related increase of water density $\Delta\rho_{SPM}$ with the following relationship:[30]

$$\Delta\rho_{SPM} = \mathrm{SPM}*(1\text{-}1/2.56).$$

Water density (ρ): Density is a basic physical property of matter. In water bodies, vertical density gradients are responsible for stable stratification. The density of water depends on its T, as well as salinity and SPM. Hence, T and $EC_{25°C}$ values as well as a Turb/SPM relationship can be used to estimate water density by applying the empirical equation of state.[30]

Depth profiles of physico-chemical parameters (*i*): Depth profiles $i(d, t)$ were derived in 1 m depth intervals on a daily basis for all physico-chemical parameters *i* but PAR. Therefore, mean values and corresponding standard deviations were calculated from the selected MINIBAT data around Xiakou.

Vertical gradients ($\delta_z i$): Vertical gradients $\delta_z i = i_d/i_{d+1\,m}$ were derived from the daily depth profiles of physico-chemical parameters *i*. From water density estimates based on T, $EC_{25°C}$, and Turb, we further calculated the vertical density gradients $\delta_z\rho$ as a measure of stratification intensity. Relationships of abs($\delta_z i$) with $\delta_z\rho$ were determined with both Pearson and Spearman correlation coefficients.

Temporal variability (var_i): We applied the commonly used squared difference approach to calculate temporal variability of physico-chemical parameters (not for PAR). For each depth *d*, the squared differences of *i* from day *n* to day *n*+1 were therefore calculated:

$$var_i = [i_n(d)\text{-}i_{n+1}(d)]^2.$$

We intended to define a comprehensive general measure of temporal variability of physico-chemical properties in the water body around Xiakou. Therefore, var_c was introduced as a dimensionless comprehensive variable incorporating var_i of the different parameters *i*. To achieve similar comparable value distributions of var_i across different parameters *i* and across all four analysed hydrological scenarios these var_i datasets required standardization. As standardization method we applied an adapted z-transformation[31] by using the robust distribution measures Median (med) as well as interquartile range r_{iq} for each individual parameter *i*:

$$var_{i\text{-}std.} = [var_i\text{-}\mathrm{med}(var_i)]/[r_{iq}(var_i)].$$

The squared differences var_i are non-negative. Therefore, it is reasonable to simply sum up their standardized values $var_{i\text{-}std.}$ for each depth *d* and day interval *n*/*n*+1 to receive var_c as a comprehensive variable of temporal physico-chemical variability in the water:

$$var_c = \Sigma_i var_{i\text{-}std.}.$$

Further, we calculated Pearson and Spearman correlation coefficients of all var_i with var_c for each fieldtrip individually to

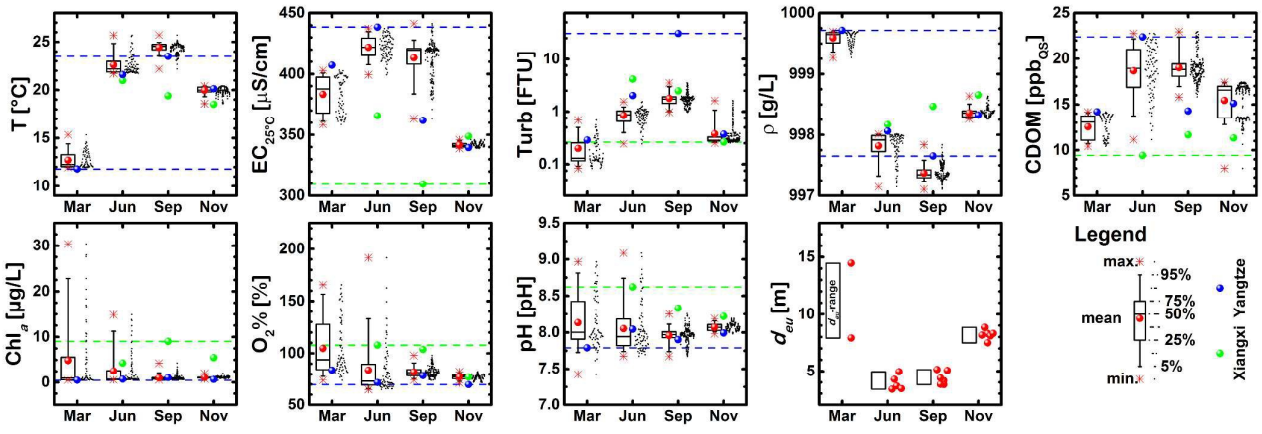

Fig. 5 Seasonal distribution plots of nine analysed characteristic parameters of the water body around Xiakou in the Xiangxi River backwater of the TGR. The corresponding source water conditions (not d_{eu}) are given for the Xiangxi River and the Yangtze River main stream. Corresponding minimum and maximum source water conditions are marked with dashed lines. Note: there is a logarithmic scale for Turb and the d_{eu} boxes represent the full value range.

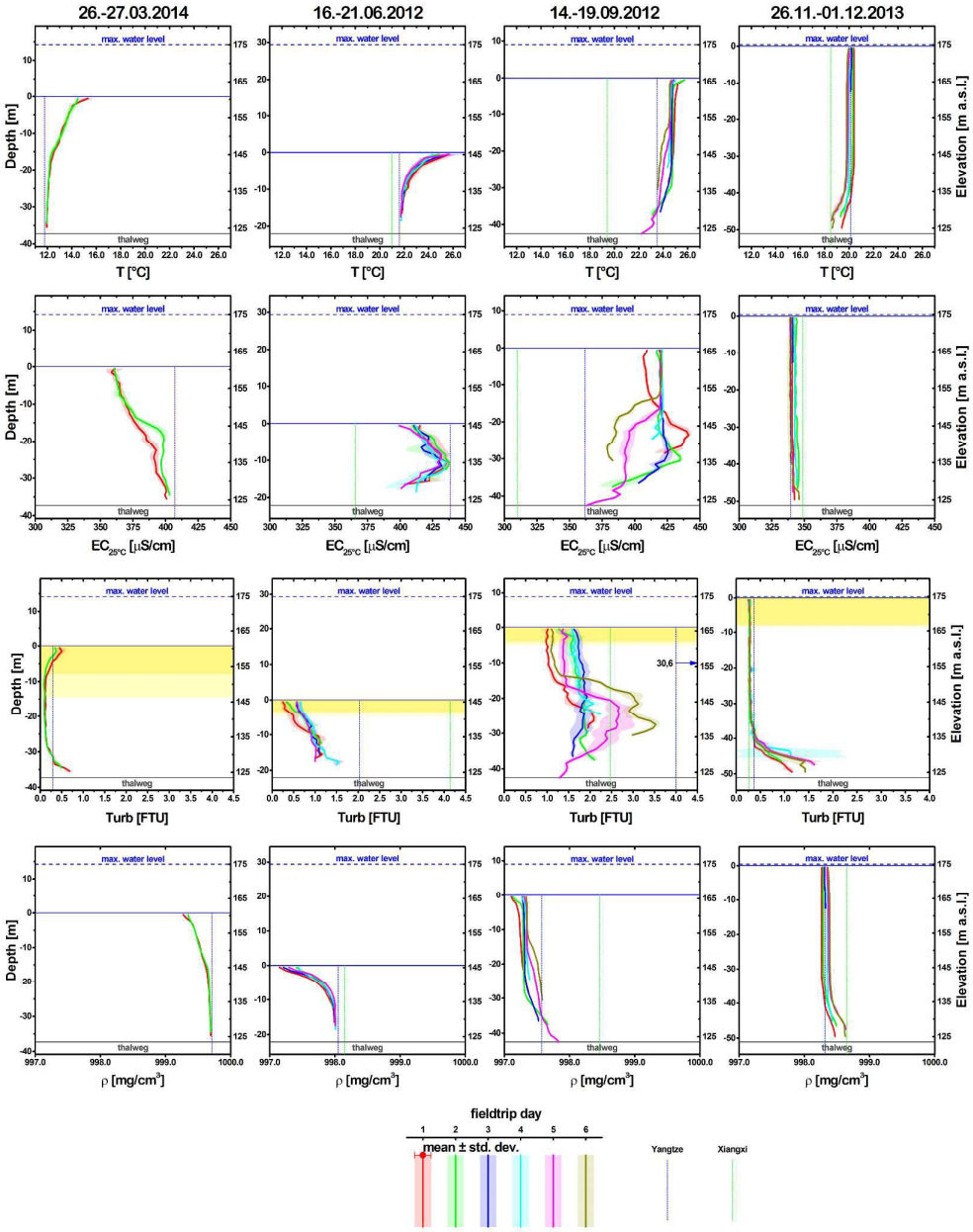

Fig. 6 Daily depth profiles of four out of eight analysed physico-chemical parameters i±σi around Xiakou in the Xiangxi River backwater of the TGR during our four fieldtrip times. d_{eu} is marked yellow in the Turb graphs, because Turb affects light attenuation (Fig. 8). Source water conditions are marked by vertical dashed lines.

extract contributions of single physico-chemical parameters *i* to var_c.

3. Results

3.1. Water density

From 107 water samples derived from all four fieldtrips, we found a strong linear relationship between log(Turb) and log(SPM) (Fig. 4). Therefore, we could estimate water density based on T, Sal (estimated from $EC_{25°C}$), and SPM (estimated from Turb) using the empirical equation of state.[30] Water density differences in the study are ranged between 997.1 and 999.7 mg/cm^3. According to these results, 97.7% of water density variations in the water body around Xiakou depended on T, whereas only 1.8% and 0.5% were related to Sal, respectively SPM. This is in accordance with prior findings for the same area.[32]

3.2. Physico-chemical parameter distributions under the four different but typical hydrological scenarios

All distributions of the analysed parameters *i* characterising the water body around Xiakou are displayed in Fig. 5 in their seasonal order. Around Xiakou, parameter distributions

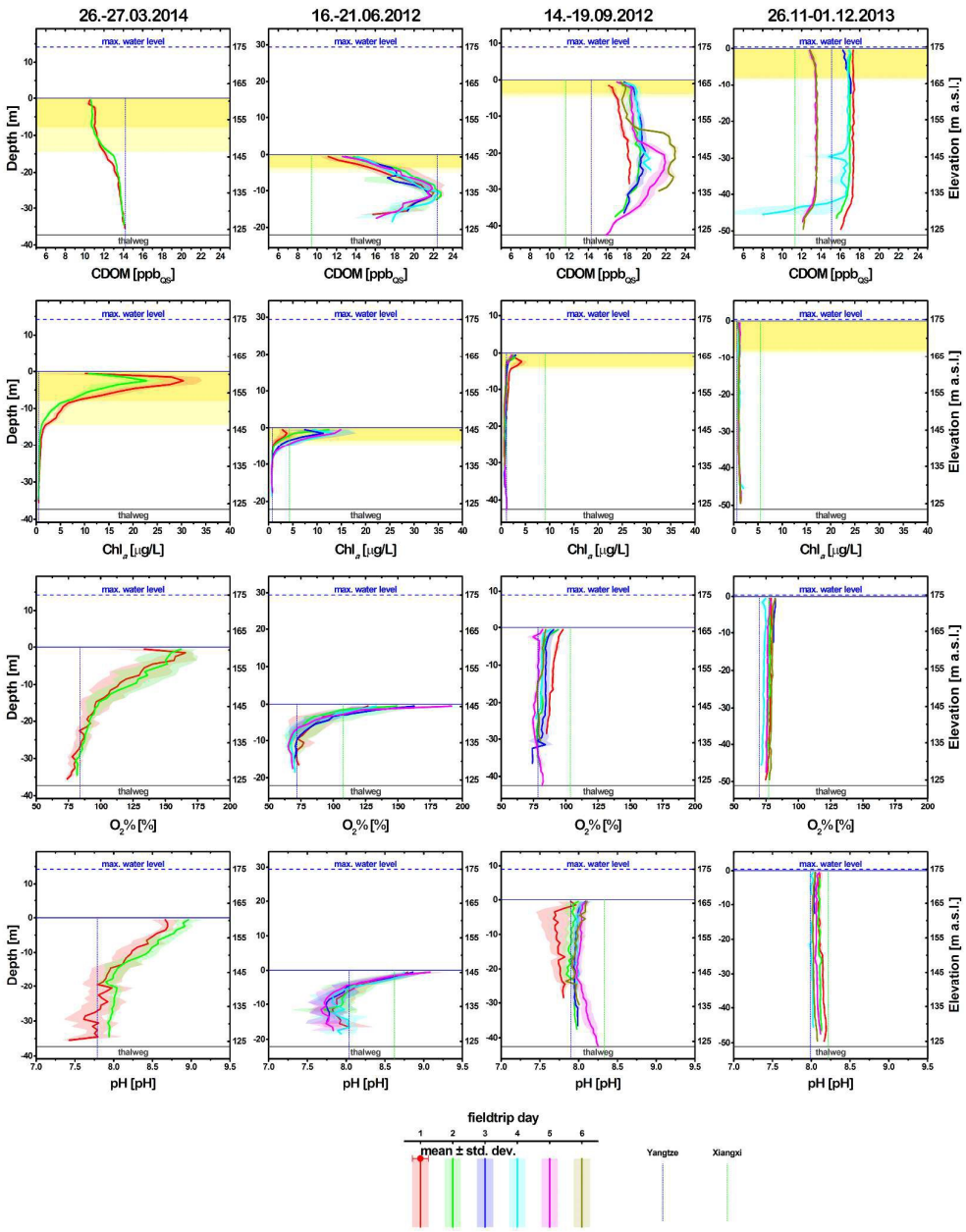

Fig. 7 Daily depth profiles of four out of eight analysed physico-chemical parameters $i \pm \sigma_i$ around Xiakou in the Xiangxi River backwater of the TGR during our four fieldtrip times. d_{eu} is marked yellow in the CDOM and Chla graphs, because CDOM affects light attenuation (Fig. 8) and algal growth depends on light conditions. Source water conditions are marked by vertical dashed lines. (continued).

exhibited three general seasonal patterns: 1) T, $EC_{25°C}$, Turb, and CDOM have a peak in June/September and lower values in March/November. ρ and d_{eu} have an opposed pattern. Chl$_a$, O_2%, and pH reached highest values in March/June and lower values in September/November. Median pH values ranged around 8.0 and it is noteworthy, that O_2% never dropped below 69% staying far away from anoxic conditions.

The Yangtze River main stream exhibited a strong seasonality for the parameters T, $EC_{25°C}$, Turb, ρ, and CDOM (Fig. 5). In general, the conditions around Xiakou in the Xiangxi River backwater followed these seasonal trends. Seasonality of the same parameters in the Xiangxi River source water was different but less pronounced and the patterns are not clearly mirrored within the Xiangxi River backwater conditions. The maximum range of source water conditions did border the conditions around Xiakou for $EC_{25°C}$ and CDOM. Only some scattered extreme values slightly exceeded these borders. T and ρ considerably exceeded the range of source water conditions in June and in September. The majority of Turb values around Xiakou were below the source water conditions. In March and June, Chl$_a$, O_2%, and pH in the water body

around Xiakou by far exceeded the source water conditions in positive direction.

3.3. Depth profile characteristics of physico-chemical parameters

Depth profiles of physico-chemical parameters in the water body around Xiakou considerably differ across the four hydrological periods covered by MINIBAT measurements (Fig. 6, Fig. 7). First of all, thermal density stratification (T and ρ) was present under all four hydrological scenarios. The main stratification in March and June was attributed to the upper water body, whereas it appeared near the thalweg in September and November.

In March and June, the depth profiles of T, $EC_{25°C}$, Turb, ρ, and CDOM showed little daily variation across the corresponding fieldtrip periods. In September, however, all these four parameters revealed considerable shifts, particularly in the middle of the water column. Within the November scenario, there were considerable shifts to lower T and CDOM that affected the whole water column.

The bottom water conditions around Xiakou in March were very similar to those of the Yangtze River main stream (T, $EC_{25°C}$, ρ, CDOM, Chl_a, O_2%, and pH). In June, it was the middle water layer that represented the Yangtze River main stream conditions (T, $EC_{25°C}$, ρ, CDOM, Chl_a, and O_2%), whilst we observed significant shifts of physico-chemical conditions (T, $EC_{25°C}$, Turb, O_2%, and pH) in the middle water layer towards the Yangtze River main stream conditions in September. Interestingly, CDOM concentrations in the middle water layer increased at the same time and moved away from both Yangtze River main stream and Xiangxi River headwater water conditions.

In March, June and November we found highest Turb values near the thalweg, only in September Turb reached its highest values in the middle water layer. In November, we observed increasing Turb and decreasing CDOM values near the thalweg below the thermocline. There was a shift of T and CDOM towards values similar to the Xiangxi River source water after 29 November, the fourth fieldtrip day. Furthermore, T and CDOM shifted towards lower values across the whole 50 m water column from 29-30 November, the fourth and fifth fieldtrip days.

The depth profiles of Chl_a, O_2%, and pH were closely related with each other during both March and June scenarios (Fig. 7). Distinct peaks of all three parameters appeared near the water surface within the euphotic zones when there were also strong thermal density stratifications present.

It is remarkable that the strongest stratification was present in June when there were the lowest water levels and second highest discharge conditions (Table 1). Further, the weakest stratification occurred in November, when water levels were highest and discharge conditions lowest (Table 1).

3.4. Dependencies of euphotic depth

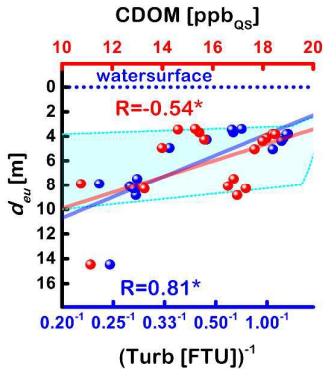

Fig. 8 Scatterplots of mean(CDOM) and mean(Turb)$^{-1}$ within the euphotic zone versus euphotic depth (d_{eu}). Lines represent least squares linear fit curves. Both Pearson correlation coefficients (R) are significant at a 0.05 level. The blue shaded area represents the range of Turb~d_{eu} relation from a study for the same area in 2009/2010 by.[4]

Algal growth depends to a large extent on the light environment near the water surface. Turb, CDOM, and algae themselves in the surface water can cause significant light attenuation and thus reduce d_{eu}. Here, we found significant negative relationships of both Turb and CDOM in the euphotic zone with d_{eu} (d_{eu}~-CDOM; d_{eu}~Turb^{-1}) (Fig. 8). For Chl_a this was not the case.

3.5. Density stratification and vertical physico-chemical gradients

As already stated in section 3.1, T was the main driving factor of water density variations in the studied water body. Therefore, abs(δ_zT) exhibited very strong correlations with δ_zρ during all analysed scenarios (Table 2). By far, the strongest vertical density gradients in the water body around Xiakou were present near the water surface in June (Fig. 9). In March and June, maximum gradients of δ_zρ were attributed to the water surface and correlated with abs($\delta_z Chl_a$), abs($\delta_z O_2$%), and abs(δ_zpH) (Table 2). In September, there are three peaks of δ_zρ along the depth profile at the water surface, in the middle water layer, and near the thalweg. These were mainly related to abs($\delta_z EC_{25°C}$), abs(δ_zTurb), and abs(δ_zCDOM) (Table 2). In November, we found highest δ_zρ values near the bottom being correlated with abs(δ_zTurb) (Fig. 9, Table 2).

3.6. Temporal variability of physico-chemical conditions in the water body around Xiakou

By far, the highest var_c values were present near the water surface in March and June (Fig. 9). In these seasons, var_T, var_{Turb}, var_{Chla}, and $var_{O2\%}$ contributed most to var_c (Table 3). In September the maximum var_c values appeared in the middle water layer and correlation was strongest with var_T, $var_{EC25°C}$, var_{Turb}, and var_{CDOM}. During the November scenario, var_c showed a relatively uniform distribution across the whole depth profile with only a slight peak near the thalweg. Correlation was strongest with var_{CDOM} and var_{pH}.

Table 2 Seasonally distributed Pearson and Spearman correlation coefficients of absolute physico-chemical vertical gradients abs($\delta_z i$) with vertical water density gradients $\delta_z\rho$ of the water body around Xiakou. Coefficients >0.5 and >0.7 are marked yellow and green, respectively.

abs($\delta_z i$)	Mar		Jun		Sep		Nov	
	Pears.	*Spear.*	*Pears.*	*Spear.*	*Pears.*	*Spear.*	*Pears.*	*Spear.*
$\delta_z T$	1.00	1.00	1.00	1.00	1.00	0.99	1.00	0.85
$\delta_z EC_{25°C}$	0.22	0.48	0.01	-0.11	0.68	0.66	0.25	0.44
δ_zTurb	0.01	-0.10	0.00	0.12	0.33	0.50	0.83	0.61
δ_zCDOM	0.44	0.39	0.56	0.46	0.42	0.60	0.28	0.46
$\delta_z Chl_a$	0.76	0.88	0.71	0.84	0.26	0.35	0.31	0.34
$\delta_z O_2$%	0.72	0.83	0.92	0.90	0.39	0.40	0.08	0.22
δ_zpH	0.26	0.52	0.89	0.80	0.19	0.17	0.05	-0.12

4. Discussion

The synopsis of our broad resulting dataset reveals fundamental environmental characteristics of the water body around Xiakou, in particular those related to the distinct and unique typical seasonal hydrology of the TGR.

4.1. Environmental conditions for algae in the Xiangxi River backwater

Basically, algae rely on a suitable range of T as well as sufficient supply with nutrients and light. Algal blooms have turned out to be the most obvious and primarily most disturbing water quality issue in the TGR. By now, it is obvious that algal blooms in the TGR are mainly not limited by nutrient availability[4,25,33] but by temporally occurring optimal stratification[4,16,34,35] and light environment conditions[4] near the water surface.

We have found the highest Chl_a, O_2%, and pH values of our study within the surface waters in March and June (Fig. 5, Fig. 7). Further, their vertical gradients also correlate with density stratification during these both scenarios (Table 2), while Chl_a, and O_2% were also amongst the parameters contributing most to temporal variability of physico-chemical conditions (Table 3). These parameters are all closely related to algae content as well as photosynthetic activity and consequently indicate a strong impact of algae on the physico-chemical conditions and dynamics within the surface water layers in March and June (Fig. 9 b). What are the specific reasons for that?

First of all, water being warmer and having much lower density than the source waters (Fig. 5) was present at the water surface (Fig. 6) in March and June. This was forming a water package being stably isolated from the flow and mixing processes possibly taking place below. Further, we found negative correlation of d_{eu} with Turb (Fig. 8). This indicates that Turb affects light availability for algae. A similar range for this relationship was found in the same area around Xiakou for the years 2009/2010.[4] Additionally, our results provide evidence that also CDOM is limiting the light availability in the studied water body (Fig. 8). Highest CDOM and Turb values occurred in June and September and were particularly enhanced within those water layers dominated by the Yangtze River main stream conditions (Fig. 7, Fig. 9 b). The high Turb values are related to excessive SPM loads of the Yangtze River main stream during the rainy season, whereas high CDOM contents are very likely to originate from urban sewage of the town Guojiaba near the confluence zone of the Xiangxi River with the Yangtze River. Corresponding evidence was provided in a former study analysing pollutant transport phenomena in the Xiangxi River backwater during the September scenario in detail.[9]

Based on our results, the conditions in March were most favourable for algal growth because the surface water was stably stratified and lowest Turb values and CDOM concentrations allowed for deep and sufficient light infiltration. This is in very good accordance with the fact that Chl_a concentrations also showed their maximum in March.

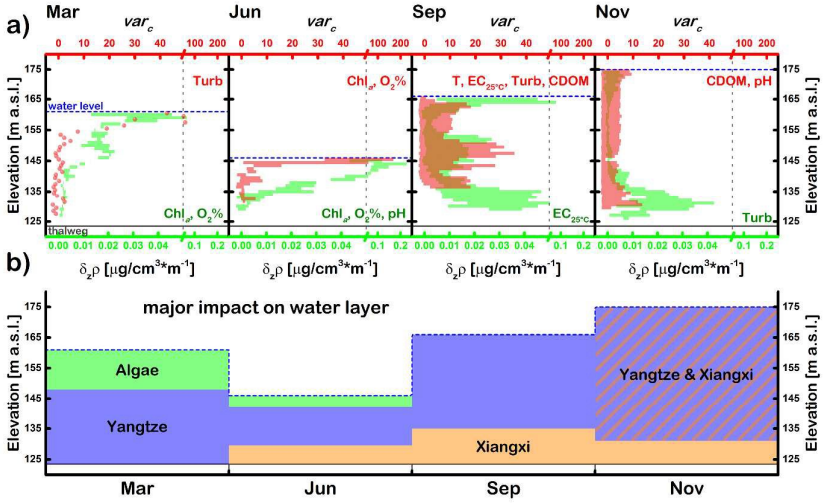

Fig. 9 a) Seasonal ranges of temporal variability var_c and vertical water density gradients $\delta_z\rho$ along depth profiles in the water body around Xiakou. Corresponding correlating physico-chemical parameters are plotted explicitly when both Spearman and Pearson correlation coefficients were > 0.5 (Table 2 and Table 3). Note: Both horizontal axes have a scale break indicated by vertical dashed lines. **b)** Derived major impacts on physico-chemical conditions in distinguishable water layers across seasons.

Table 3 Seasonally distributed Pearson and Spearman correlation coefficients of temporal variability var_c with individual squared differences var_i of physico-chemical parameters *i* in the water body around Xiakou. Coefficients >0.5 and >0.7 are marked yellow and green, respectively.

var_i	Mar		Jun		Sep		Nov	
	Pears.	*Spear.*	*Pears.*	*Spear.*	*Pears.*	*Spear.*	*Pears.*	*Spear.*
var_T	0.42	0.21	0.95	0.32	0.84	0.55	0.49	0.33
$var_{EC25°C}$	-0.26	0.15	0.27	0.02	0.88	0.76	0.32	0.48
var_{Turb}	0.94	0.61	0.08	0.16	0.94	0.85	0.34	0.34
var_{CDOM}	0.01	0.08	0.05	0.15	0.84	0.79	0.87	0.72
var_{Chla}	0.88	0.37	0.78	0.71	0.22	0.07	0.29	0.34
$var_{O2\%}$	0.52	0.48	0.97	0.59	0.25	0.36	0.07	0.21
var_{pH}	0.25	0.20	0.42	0.13	0.35	0.43	0.67	0.68

4.2. Contributions to dissolved and particulate water constituents

4.2.1.The main actor: Yangtze River main stream

From Fig. 5 it becomes apparent that under the observed normal hydrological scenarios the Yangtze River was the main driving factor for the seasonality of a number of physico-chemical parameters (T, $EC_{25°C}$, Turb, ρ, CDOM) in the water body around Xiakou. The distributions of these parameters generally follow the Yangtze River main stream conditions. In particular, dissolved (indicated by $EC_{25°C}$ and CDOM) and particulate (indicated by Turb) water constituents are mainly derived from the Yangtze River main stream. Further, our results imply that September was the scenario most relevant for water mass exchange between the Yangtze River main stream and the Xiangxi River backwater. This becomes obvious from the changing depth profile characteristics of $EC_{25°C}$, Turb, and CDOM as well as from the large contributions of $var_{EC25°C}$, var_{Turb}, and var_{CDOM} to the total temporal variability of physico-chemical properties var_c in September (Table 3). Maximum var_c values in this season appeared in the middle water layer (Fig. 8). As we have seen in a former study[9] this layer was affected by a massive interflow density current intrusion from the Yangtze River main stream after considerable water level rise in the TGR. Even 20 km upstream within the Xiangxi River backwater we were subsequently able to observe corresponding radical changes of physico-chemical properties within only some days. Amongst large reservoirs worldwide, the TGR is unique in terms of its immense water level fluctuation (section 1). Indeed, this unique property is forming an enormous tidal pump between the Xiangxi River backwater and the Yangtze River main stream. Rising water levels in the TGR Yangtze River main stream induce a net upstream flow into tributary backwaters as long as inflows from the tributary headwaters are not extremely high. E.g. around the September scenario when TGR water level was rising by 6 m the additional water volume of the Xiangxi River backwater was contributed almost equally by both, headwater inflows and water from the Yangtze River main stream.[9] This tidal pump is further amplified by the formation of density current circulation cells.[4,9] Pollutant fluxes, explicitly including nutrients and heavy metals, from the Yangtze River main stream into the Xiangxi River backwater thus appear to be mainly attributed to the rising water level period in autumn. A recent study has shown that Phosphorus and Nitrogen input from the Yangtze River main stream into the Xiangxi River backwater amount to 80% respectively 60% of the backwater's nutrient balance.[18] In this study, total phosphorus concentrations from April till August ranged between 0.17 µg/L and 0.3 µg/L whereas from September till December these were below 0.13 µg/L. Further, high loads of particle bound heavy metals have been transported into the Xiangxi River backwater during the September scenario.[9] Generally, large amounts of nutrients and heavy metals in the TGR occur being bound to particles.[9,14,18] Hence, Turbidity signals from the Yangtze River main stream within the Xiangxi River backwater are an obvious indication of corresponding particle related pollutant transport.

4.2.2.The Xiangxi River headwater: taking its chance in winter

The comparison of physico-chemical conditions in the Xiangxi River headwater with depth profiles in the water body around Xiakou reveals obvious impacts of the Xiangxi River headwater conditions to the bottom water layer in June ($EC_{25°C}$, CDOM) September (T, ρ, pH), and November (T, ρ, CDOM) (Fig. 6, Fig. 7, Fig. 9). In June and September these obvious impacts remain strongly limited to the bottom water and do not seem to significantly interfere with overlaying water. In November, however, water masses with low concentrations of CDOM appeared near the thalweg on 29 November and were rapidly mixed with the above water column causing marked reduction of CDOM concentration there as well (Fig. 7). This fact is also expressed in the large contribution of var_{CDOM} to var_c in November (Table 3). The rapid distribution of changing CDOM across the whole water column that originated from the bottom layer can be regarded as a tracer for any dissolved substances. During the high water level period, changes of water characteristics in the bottom water layer can rapidly alter the physico-chemical properties of the whole water column around Xiakou as there is nearly no thermal density stratification present in the upper water layers. Even though the contribution of the Xiangxi River headwater to the total nutrient balances of the backwater is comparably low, concentrations in the tributary headwater can be temporally very high.[33,34,18] As such, introduced pollutants from the upstream water bodies can seriously contribute to nutrient concentrations in the Xiangxi River backwater during the high water level period in winter.

4.3. The backwater of the Xiangxi River as temporal buffer of physico-chemical properties

The range of $EC_{25°C}$ values in the water body around Xiakou is bordered by the source water conditions (Fig. 5). This is an evidence for conservative water mass mixing processes between the Yangtze River main stream and the Xiangxi River headwater. Further, from $EC_{25°C}$ in Fig. 5 a strong temporal water quality buffer capacity of the Xiangxi River backwater can be derived. The seasonal sequence of $EC_{25°C}$ in the Yangtze River main stream appears to spearhead $EC_{25°C}$ parameters in the Xiangxi River backwater (Fig. 5). In September, the majority of $EC_{25°C}$ values fit well into the range of the preceding June event. Both source waters in September, however, revealed much lower $EC_{25°C}$. Obviously, the water around Xiakou still

contained the dissolved solids from the preceding summer season. Water residence times in the tributary backwaters of the TGR can be greater than 365 days[36] and by far exceed the maximum of 81 days that we calculated for the whole TGR. Thus, water that once enters a TGR tributary backwater can stay there for a long time retaining some stable physico-chemical characteristics whilst the conditions in its source waters might change considerably. This finding is of particular interest regarding pollutants (e.g. nutrients) that enter the Xiangxi River backwater during the rising and high water level periods. Nutrients as an example can derive from both the Yangtze River main stream (section 4.2) and the Xiangxi River headwater (section 4.2.2) and will be retained within the backwater. As such eutrophication problems in the spring and summer periods are seriously driven by nutrient transport dynamics in the preceding autumn and winter seasons. Due to the fact that algal blooms in the TGR are mainly not limited by nutrients,[4,25,33] we propose that the effective nutrient transportation processes from the Yangtze River main stream into its tributary backwaters are the most prominent reason for algal blooms in the TGR. According to our results, this transport is mainly taking place within the autumn season which has attracted little attention by environmental scientists, so far. Further, regarding the seasonality of Turb distributions (Fig. 5) provides evidence for sedimentation processes taking place within the Xiangxi River backwater. The majority of Turb values fall below the simultaneously prevailing Turb conditions of both source waters with minimum values being reached in March. Hence, SPM concentrations in the water column must be decreasing due to sedimentation. As a consequence, contaminated particles entering into the backwater during the rising water level phase, as it was the case during the September scenario,[9] are very likely to settle down and accumulate within the sediments and semi-terrestrial soils of the water level fluctuation zone. This possible creeping environmental threat to sediment and semi-terrestrial soil quality is, however, only insufficiently studied, yet.

4.4. The observed effects put into a general context

Indeed, the observed effects of water mass interactions and their environmental impacts for the TGR and its major tributary backwater of the Xiangxi River are not totally new in themselves. The distribution of pollutants from inflowing waters into stratified water bodies is closely linked to the formation of corresponding density currents and vertical mixing processes.[37] In particular, the availability of nutrients to algae near the water surface requires appropriate water body conditions. Further, pollutants within the particulate phase are also likely to be withdrawn from the water column by sedimentation.[37]

The investigated area of this study revealed a complex interacting system of two separate inflows. Pathways of multiple gravitational inflows into a stratified reservoir in Australia have already been studied.[38] Each inflow influenced the physico-chemical structure of the stratified water body according to its density and volume flux in downstream direction. In this respect, we are dealing with an exceptional case, here. The flow directions are not solely linear from upstream to downstream. On the one hand, inflows from the Xiangxi River headwater form an ordinary underflow constantly moving downstream (Fig. 6, Fig. 7, and Fig. 9). On the other hand water from the Yangtze River main stream is forming intrusions moving upstream as an underflow (June) or interflow (September) into the dendritic tributary backwater. Further, the intensity of this intrusion is driven by both gravitational forces and the tidal pump caused by TGR water level fluctuations (section 4.2.1). It is obvious from the physico-chemical characteristics (Fig. 6, Fig. 7) that the intruding waters of both inflows also reach the surface of the tributary backwater in autumn and winter (Fig. 6, Fig. 7, and Fig. 9). As tracer experiments in a Spanish stratified reservoir have shown, this can happen very rapidly by partial mixing at the interface between the density current and the overlying water.[39] Particularly when a density current intrusion enters right below the surface mixed layer corresponding tracers could quickly reach the water surface as well.[39] This was the case here in both September and November scenarios. As such, dissolved nutrients originating from either the Xiangxi River headwater or the Yangtze River main stream are very likely to reach the surface water layer and aggravate eutrophication problems, there.

Under normal hydrological conditions, the Yangtze River's major role in providing dissolved and particulate water constituents to the Xiangxi River backwater becomes obvious from our data. The same fact is also known for nutrients.[18] Further, the TGR exhibits an exceptional flow and mixing pattern with its tributary backwaters which happens to be strongly linked to the enormous annual TGR water level fluctuation. Consequently, major parts of the current pollution within its tributary backwaters can be attributed to the TGR water level fluctuation, being its outstanding and unique feature in a global context.

5. Conclusions and recommendations for water quality control

Under the observed normal hydrological conditions in the TGR, we found seasonally very different environmental water body characteristics around Xiakou in the Xiangxi River backwater. The falling and low water level phases were characterized by pronounced thermal density stratification near the water surface and went along with high algal abundance that dominated major physico-chemical conditions and dynamics. The rising water level season in September was characterized by radical changes of physico-chemical properties within only some days driven by inflowing water from the Yangtze River main stream. During the high water level period in November, underflowing water from the Xiangxi River headwater was able to rapidly alter the physico-chemical conditions of the whole upper water column as there was nearly no thermal density stratification present.

The Yangtze River main stream appeared to be the main driver of dissolved and particulate water constituents within the Xiangxi River backwater. As such it is also the main contributor of pollutants to this water body. This is particularly serious as we also identified an enormous physico-chemical buffer capacity of this tributary backwater. Hence, nutrients entering from the Yangtze River main stream into the Xiangxi River backwater during the rising water level period can still be available to algae in the following spring and summer seasons.

As highlighted in the 'Introduction', the TGR is globally unique due to its enormous annual water level fluctuation scheme. The results of this study have provided evidence that this water fluctuation itself has become a central part of the recent eutrophication and pollution problems in the TGR, particularly within its tributary backwaters. Surely this phenomenon is not limited to the Xiangxi River backwater because it is symptomatic for the TGR that the Yangtze River main stream is characterized by higher pollution levels than its tributaries.[19,40] It is also obvious that similar processes of varying magnitude do and/or will occur in reservoirs worldwide. Therefore, this study provides adequate monitoring strategies and a database to be built on. Again, it is noteworthy that our study did only cover 'normal' hydrological scenarios related to the typical and systematic water level changes induced by the TGD management. Exceptional extreme events may rapidly alter this described interacting system between the Yangtze River main stream and its tributary backwaters very seriously.

Are there now any ways to mitigate the current 'normal' situation?

Controlled water level fluctuations in the TGR are seriously considered an effective way to mitigate algal blooms in TGR tributary backwaters.[4,25] Therefore, strong turbulences near the water surface should be induced by artificial water level fluctuations in the TGR (TGD management) and cause the collapse of stable thermal density stratification at the water surface. From the perspective of our study such an approach seems plausible to mitigate threats by algal blooms alone. But, it is not capable to reduce the pollutant inputs from the Yangtze River main stream into its tributary backwaters. To account for this as well, the rising water level phase of the TGR would require feedback with pollutant concentrations in the Yangtze River main stream. Within the frame of guaranteed flood protection, we therefore propose, that the TGR should only be filled up when pollutant/SPM concentrations in the Yangtze River main stream have dropped below some thresholds after the summer rainy season. How to specify this suggestion? Major nutrient[14] and heavy metal[9] fractions are to be found within the SPM and contents of SPM in the Yangtze River main stream generally drop very rapidly after the flood season in summer. For instance, in their study Yang et al. (2015)[18] identified highest total phosphorus concentrations around 0.3 µg/L in the Yangtze River main stream in late August 2013 when water levels in the TGR already started to rise (Fig. 2). Just one month later they measured lowest total phosphorus concentrations of 0.1 µg/L. In this case, a slight delay of the rising water level period would have drastically reduced phosphorus input into the Xiangxi River backwater by intruding water masses from the Yangtze River main stream.

Further, a more gentle rise of the water level in autumn could also reduce particle transport distances upstream into tributary backwaters due to their earlier sedimentation. As discussed above, transport processes from the Yangtze River main stream appear to be mainly linked to water level fluctuations and to the formation of corresponding density current cells. Our proposal is thus only capable to reduce the pollutant transport directly linked to water level fluctuations. Other processes will remain active and a general reduction of the current pollution state still needs to be the primary long-term goal. We are aware that the TGR water level fluctuation scheme was optimised for two of its primary goals, flood protection and power generation. Our proposed approach would obviously require increasing monitoring efforts, flexibility of the TGD management, and would lead to some deficiencies in power generation. Still, it might help to mitigate the spatial range of pollution and eutrophication within the precious and most vulnerable TGR tributary backwaters. It is similarly applicable to dendritic reservoirs worldwide, where comparable effects of varying magnitude can occur.

Acknowledgements

This research was funded by the Federal Ministry of Education and Research of Germany (BMBF grant no. 02WT1131), the National Natural Science Foundation of China (31123001), the China Three Gorges Corporation (0711442), and the International Science and Technology Cooperation Program of China (MOST grant no. 2007DFA90510).

Notes and references

1 C. Nilsson, C. A. Reidy, M. Dynesius and C. Revenga, *Science*, 2005, **308**, 405–408.
2 M. Ponseti and J. López-Pujol, *HMiC: Història Moderna I Contemporània*, 2006, 151–188.
3 Ministry of Environmental Protection of the People's Republic of China, *Three Gorges Bulletin in 2011*, 2012, url: http://english.mep.gov.cn.
4 L. Liu, D. Liu, D. Johnson, Z. Yi and Y. Huang, *Water Research*, 2012, **46(7)**, 2121–2130.
5 International Commission on Large Dams, *World Register of Dams*, 2014, url: http://www.icold-cigb.org (accessed September 22, 2014).
6 International Energy Agency, *China, People's Republic of: Indicators for 2012, Statistics*, 2014, url: http://www.iea.org (accessed September 22, 2014).
7 B. Fu, B Wu, Y Lü, Z Xu, J Cao, D Niu, G Yang and Y Zhou, *Prog. Phys. Geogr.*, 2010, **34(6),** 741-754.
8 X., Yang and X. Lu, *Environ. Res. Let.*, 2013, **8**, 1–5.
9 A. Holbach, S. Norra, L. Wang, Y. Yuan, W. Hu, B. Zheng and Y. Bi, *Environ. Sci. Technol.*, 2014, **48(14)**, 7798–7806.
10 J. Lin, C. Fu, X. Zhang, K. Xie and Z. Yu, *Biol. Trace Elem. Res.*, 2012, **145**, 268–272.
11 C. Ye, S. Li, Y. Zhang and Q. Zhang, *J. Hazard. Mater.*, 2011, **191(1–3)**, 366–372.
12 Z.-Y. Wang, Y. Li and Y. He, *Water Resour. Res.*, 2007, **43**, W04401.

13 Z. Yang, H. Wang, Y. Saito, J. D. Milliman, K. Xu, S. Qiao and G. Shi, *Water Resour. Res.*, 2006, **42**, W04407.
14 A. Holbach, L. Wang, H. Chen, N. Schleicher, W. Hu, B. Zheng and S. Norra, *Environ. Sci. Pollut. R.*, 2013, **20(10)**, 7027-7037.
15 Y. Xu, M. Zhang, L. Wang, L. Kong and Q. Cai, *Quat. Int.*, 2011, **244**, 272-279.
16 Z. Yu and L. Wang, *J. Hydrodyn. Ser. B (English Ed.)*, 2011, **23(4)**, 407-415.
17 L. Dai, H. Dai and D. Jiang, *J. Food Agric. Environ.*, 2012, **10(2)**, 1174-1178.
18 L. Yang, D. Liu, Y. Huang, Z. Yang, D. Ji and L. Song, *Ecol. Eng.*, 2015, **77**, 65-73.
19 Y. Huang, P. Zhang, D. Liu, Z. Yang and D. Ji, *Environ. Monit. Assess.*, 2014, **186(10)**, 6833-6847.
20 H. Dai, J. Mao, D. Jiang and L. Wang, *PLoS ONE*, 2013, **8(7)**, e68186.
21 J. Li, Z. Jin and W. Yang, Ecol. Inform., 2014, **22**, 1574-9541.
22 D. Stüben, K. Stüben and P. Haushahn, *Underwat. Syst. Des.*, 1994, **16**, 5–14.
23 S. Becker, M. Gemmer and T. Jiang, *Stoch. Env. Res. Risk. A.,* 2006, **20**, 435–444.
24 China Three Gorges Corporation, 2014, url: http://cwic.com.cn/inc/sqsk.php (accessed October 10, 2014).
25 Z. Yang, D. Liu, D. Ji, S. Xiao, Y. Huang and J. Ma, *Sci. China Technol. Sc.,* 2013, **56(6)**, 1458-1470.
26 United States Department of the Interior, *National Irrigation Water Quality Program Information Report No.3*, 1998.
27 S. P. Gloss, L. M. Mayer and D. E. Kidd, *Limnol. Oceanogr.,* 1980, **25**, 219-228.
28 N. Hudson, A. Baker and D. Reynolds, *River. Res. Applic.*, 2007, **23**, 631–649.
29 W. Lampert and U. Sommer, *Limnoökologie*, 1999.
30 Z.-G. Ji, *Hydrodynamics and water quality: modeling rivers, lakes, and estuaries*, 2007.
31 J. Bortz, *Statistik für Sozialwissenschaftler (5th edition)*, 1999, Springer, Berlin (in German).
32 Z. Yang, D. Liu, D. Ji and S. Xiao, *Sci. China Technol. Sc.*, 2010, **53(4)**, 1114-1125.
33 H. Dai, J. Mao, D. Jiang and L. Wang, *PLoS ONE*, 2013, **8(7)**, e68186.
34 J. Li, Z. Jin and W. Yang, *Ecol. Inform.,* 2014, **22**, 23–35.
35 K. Zhu, Y. Bi, and Z. Hu, *Sci. Total Environ.*, 2013, **450-451**, 169-177.
36 Y. Xu, Q. Cai, M. Shao, X. Han and M. Cao, *Quat. Int.*, 2009, **208**, 138–144.
37 G. Friedl and A. Wüest, *Aquat. Sci.*, 2002, **64**, 55-65.
38 C. L. Marti, R. Mills and J. Imberger, *Ad. Wat. Res*, 2011, **34**, 551-561.
39 A. Cortés, W. E. Fleenor, M. G. Wells, I. de Vicente and F. J. Rueda, *Limnol. Oceanogr.*, 2014, **59(1)**, 2014, 233–250.
40 Z. Luo, B. Zhu, B. Zheng and Y. Zhang, *China Environmental Science*, 2007, **27**, 208–212 (in Chinese).